

Hydrogen Electrochemistry and Stress-Induced Leakage Current in Silica

Peter E. Blöchl¹ and James H. Stathis²

¹IBM Research, Zurich Research Laboratory, CH-8803 Rüschlikon, Switzerland

²IBM Research, T.J. Watson Research Center, Yorktown Heights, New York 10598

(Received 21 December 1998)

Hydrogen-related defects in oxygen-deficient silica, representing the material of a thermal gate oxide, are analyzed using first-principles calculations. Energetics and charge-state levels of oxygen vacancies, hydrogen, and their complexes in the silica framework are mapped out. The neutral hydrogen bridge, called E_4' in quartz, is identified as the trap responsible for stress-induced leakage current, a forerunner of dielectric breakdown in metal-oxide–semiconductor devices.

PACS numbers: 71.55.Cn, 72.20.-i, 73.50.-h

A major concern in silicon technology is the reliability of MOS (metal-oxide semiconductor) devices such as MOSFETs (MOS field-effect transistors) and MOSC (MOS capacitor) memory cells as they are scaled to smaller dimensions. Among the main problems are the increased gate leakage current, the reduced threshold for dielectric breakdown, and oxide charging, which results in voltage shifts. Recent extrapolations [1] indicate that the gate-oxide thickness will be limited to 2.2–2.6 nm, which interferes with the road map of the Semiconductor Industry Association within the next five years. The desire to understand the microscopic origin of the detrimental effects in MOS structures bears the hope that guided modifications of the fabrication process may yield devices that can reliably be extended to smaller structures.

Degradation of MOS structures has been attributed to hydrogen diffusing to the oxide–semiconductor interface [2,3]. In this model, hydrogen is released from the metal-oxide interface by hot electrons and diffuses to the oxide–semiconductor interface, where it de-passivates hydrogenated silicon-dangling-bond defects at the oxide–semiconductor interface, called P_b centers [4].

Recently, however, it was shown that atomic hydrogen induces defects in concentrations exceeding that of P_b centers. These hydrogen-induced defects are fast interface states [4,5] and slow states [6]. The interface-state density of hydrogen-induced states closely resembles that of hot-electron-induced states, but differs from that of P_b centers [7].

In addition, low-field leakage currents, which are considered forerunners of dielectric breakdown [8], are generated by exposure to atomic hydrogen [9]. DiMaria and Cartier [9] deduced that neutral electron traps are the dominant cause of stress-induced leakage currents (SILC). The increasing number of traps in a humid atmosphere indicates that hydrogen is part of the defect structure [10]. These still uncharacterized defects may be the main cause of the degradation of thin-gate oxides. Thus an understanding of the hydrogen chemistry of gate oxides is of utmost importance for the further scaling of semiconductor devices.

How can we identify a defect as a good candidate for causing SILC?

One requirement is charge-state levels near the Fermi level of the contacts, which is ~ 3 eV below the oxide conduction-band edge.

A second requirement is a small relaxation of the charge-state levels. A defect can contribute to the leakage current only if its charge-state level shifts upon relaxation by less than the applied voltage [11]. The principle is illustrated in Fig. 1. Large level shifts upon charging are common in silica, which combines a flexible structural network with a wide band gap. Electron tunneling from the anode to the defect can occur if the Fermi level lies at or above the charge-state level of the defect. Once charged, the defect changes its structure because it can lower the energy of the electron by deforming or reconstructing the lattice. This results in a downward shift of the, now filled, charge-state level. If this shift is greater than the applied voltage, the relaxed level lies below the Fermi level. Hence the electron cannot tunnel from the defect to the cathode, because the states of the contact at this energy are occupied: The electron is trapped. To allow tunneling of the electron to the cathode, a voltage

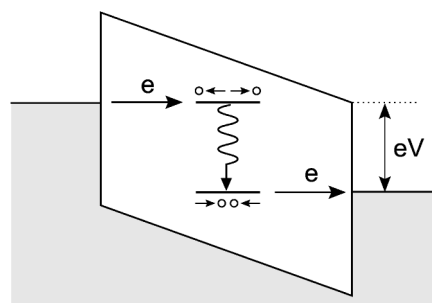


FIG. 1. Schematic representation of inelastic tunneling through a defect. Occupied states are indicated by gray background. Valence and conduction bands are sloped owing to the electric field. The electron tunnels elastically into and out of the defect level, but the defect level relaxes downward upon charging. A voltage greater than this level shift is needed to draw a current. (The band gap of the contacts has been omitted.)

larger than the level shift is required. Once the defect is uncharged, it will relax into its initial structure, placing the charging level into the original position. As a result the two-step tunneling via the defect is inelastic, and electrons lose in the form of heat an amount of energy equal to the shift of the charge-state level upon charging.

For this argument to be valid, the time to relax the structure must be shorter than the residence time of the electron on the defect. The measured leakage current [1] provides an upper and lower bound of the residence time of, respectively, 10^{-4} and 10^{-9} s in a two-step tunneling process. This is sufficiently separated from typical structural relaxation times of 10^{-13} to 10^{-12} s.

In this paper we investigate hydrogen, oxygen vacancies, and their complexes in silica. Oxygen vacancies have been considered because they are abundant in thermal oxides and because they interact with hydrogen. We evaluated structure, energetics, and charge-state levels for a comprehensive list of sixteen defects, covering interstitial molecular and atomic hydrogen, the oxygen vacancy and its complexes with one and two hydrogen atoms, their metastable states, and charge states. Charge-state levels are given in Table I and shown in Fig. 2. A detailed description of all defects will be given elsewhere. In this paper we focus on the defects relevant for SILC, and restrict ourselves to general observations regarding other defects.

Most defects in silica exhibit large level shifts, which excludes them as being the cause of SILC. Only one defect, the hydrogen bridge, satisfies all requirements for SILC. A second hydrogen-related defect, the $E'_2(E'_\beta)$ center, contributes to SILC at higher voltages (>3 eV).

Our calculations are based on density functional theory (DFT) [12] using gradient corrections [13]. Total energies and structures are calculated using the projector augmented wave method [14,15]. The calculations presented here are done in α quartz. We used a tetragonal supercell containing 24 SiO_2 formula units and having lattice constants of $(a, b, c) = (8.59, 9.82, 10.80)$ Å. A crystalline matrix has been chosen because it is a well-defined reference system for the evaluation of relative energies; thus

TABLE I. Thermodynamic charge-state level ϵ_{th} , mean value ϵ_{av} , and shift Δ of switching charge-state levels (in eV). For the switching levels between the neutral and negative charge states, $\epsilon_{\text{sw}}(0/-)$ for charging and $\epsilon_{\text{sw}}(-/0)$ for uncharging, $\epsilon_{\text{av}}(0/-)$ is defined as $[\epsilon_{\text{sw}}(0/-) + \epsilon_{\text{sw}}(-/0)]/2$ and $\Delta(0/-)$ as $\epsilon_{\text{sw}}(0/-) - \epsilon_{\text{sw}}(-/0)$. Levels are relative to the Si midgap, and lower bounds are given when shallow acceptor levels are involved.

Defect	ϵ_{th}	ϵ_{av} (+ / 0)	Δ (+ / 0)	ϵ_{av} (0 / -)	Δ (0 / -)
(SiH) ₂	-2.74 (+ / 0)	-2.37	2.60		
O vacancy	-3.03 (+ / 0)	-2.54	2.32		
Si(3) + O(3)	-0.06 (+ / 0)	-0.17	1.70		
H	0.20 (+ / -)	>-0.21	>4.10	-0.58	4.23
SiH + Si(3)	0.30 (+ / -)	>0.25	>2.92	-0.29	3.11
H bridge	0.33 (+ / 0)	0.26	2.22		
H bridge	0.74 (0 / -)			0.72	1.71

sampling over a large number of different sites is avoided. Whereas we do not expect the gross features to be affected significantly, it should be kept in mind that the amorphous matrix itself imposes strain on individual bonds.

We obtain charging levels as total energy differences, which are well defined in DFT. They are measured relative to the Si midgap level of the interface, determined empirically as shown below.

We differentiate between two charge-state levels, *thermodynamic* and *switching*. The thermodynamic level ϵ_{th} corresponds to the Fermi-level position for which the defect changes its charge state in thermal equilibrium. It is obtained from the energy difference of two relaxed configurations having different charge. Tunneling processes are nonequilibrium processes for which we define the switching levels ϵ_{sw} as the electron or hole energy required to charge or uncharge a defect according to the Franck-Condon principle. These levels are obtained from the total energy difference of two charge states in the structure of the initial charge state. Charge-state levels are denoted + / 0, 0 / -, and + / -, indicating the pair of participating charge states.

Let us first align our calculated charge-state levels with the oxide band edges. Hydrogen in the oxide near the Si/SiO₂ interface induces a characteristic peak 0.2 eV above the silicon midgap level [6,7]. Its position is independent of the sweep direction in *C-V* experiments [16]. As all relevant defects in the oxide have relaxation energies greater than 1.5 eV, this peak is therefore identified by a thermodynamic charge-state level. Furthermore, the measured number of states does not saturate with hydrogen exposure, and greatly exceeds the number of silicon dangling-bond defects in the oxide and at the interface, the so-called E' and P_b centers. This indicates that the states

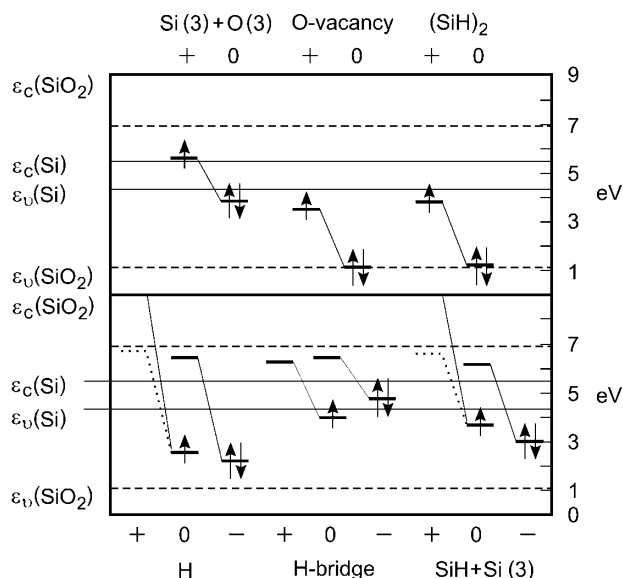


FIG. 2. Switching charge-state levels ϵ_{sw} . Dashed lines indicate the DFT band edges. Dotted lines indicate the DFT position of shallow acceptor levels. See text and Table I for explanations.

are related to hydrogen interacting with the unperturbed silica framework. Our calculations confirm that atomic hydrogen in silica has only a single thermodynamic charge-state level [17]. Hence, we attribute the observed state to the $+/-$ thermodynamic charge-state level of atomic hydrogen. This is the first assignment of the hydrogen-induced density of states with an atomistic model. The assignment explains why no electron paramagnetic resonance (EPR) signal could so far be associated with the electrically observed density of states despite considerable effort: Hydrogen is a negative- U defect, i.e., the neutral, EPR visible, charge state is thermodynamically unstable for all Fermi-level positions.

From this assignment we obtain an estimate of the Si midgap energy, our reference energy for the electrons relative to the calculated levels. Together with the measured valence-band offset of 4.3 eV [18] and the experimental band gap of silicon, the charge-state level of hydrogen empirically determines the oxide valence-band top to be 1.0 eV below the DFT valence-band top.

Most defects considered can be regarded as combinations of a small set of structural motifs: Dangling bonds on undercoordinated silicon atoms, denoted Si(3), are responsible for a suite of E' centers [19]. When positively charged, the undercoordinated silicon atom binds to an oxygen bridge, forming a threefold-coordinated oxygen atom, denoted O(3), which is the dominant positive-charge defect. When negatively charged, the undercoordinated silicon atom has a tendency to establish a bond to a, then fivefold-coordinated, silicon atom. Hydrogen atoms interact with the framework in an analogous manner: They bind to an oxygen when positive, and to a silicon atom when negative [17]. No bonds are established in the neutral state. Hydrogen interacts with a silicon dangling bond by forming a SiH fragment. The strong tendency for rebonding causes large level shifts upon charging, and explains the tendency of silica to undergo oxide charging.

Let us now discuss how individual defect classes can be excluded as being the cause of SILC.

The oxygen vacancy has two metastable partners [20–23]. For relevant Fermi-level positions the oxygen vacancy is neutral. Even though the metastable form of the oxygen vacancy, denoted Si(3) + O(3), which is related to the so-called E'_1 or E'_γ center [24,25], has charge-state levels in the correct energy region and exhibits only small level shifts upon charging, it overcomes a small barrier after electron capture and transforms into the stabler, direct silicon-silicon bond.

The hydrogen molecule and the complex of two hydrogen atoms with the vacancy denoted (SiH)₂ are stable as neutral species and do not contribute to SILC.

From the charge-state levels and their shifts, we identify the hydrogen bridge as the defect most likely responsible for SILC at low voltages. The neutral hydrogen bridge in quartz has been attributed to the E'_4 center [26]. We will discuss this defect in some detail.

The hydrogen bridge deviates from the structural motifs described above. In the hydrogen bridge, a hydrogen atom replaces an oxygen atom as shown in Fig. 3. Hence, it is a complex of a hydrogen atom with an oxygen vacancy.

The electronic structure of the hydrogen bridge can be rationalized in simple terms by a three-center bond of two silicon dangling bonds with the hydrogen s orbital. The completely bonding state lies in the SiO₂ valence band, and the completely antibonding combination of these orbitals lies in the SiO₂ conduction band. The nonbonding orbital lies in the gap and contains none, one, or two electrons for the positive, neutral, and negative charge states, respectively.

The occupation of this nonbonding orbital has only a minor effect on the bond strength and structure. Furthermore, the Si-H-Si bonding orbital in the valence band prevents the defect from breaking up. Thus this hydrogen bridge is exceptionally rigid in comparison to other defects in silica. The small relaxations are reflected in small shifts of the charge-state levels upon charging. When the neutral hydrogen bridge traps an electron, the level is shifted down by only 1.7 eV. This makes the hydrogen-bridge center a good candidate for the electron trap responsible for SILC. The positive-to-neutral transition may also contribute because its level shifts by only 2.2 eV.

The oxygen vacancy binds a proton with 0.5–1.5 eV depending on the charge states. Hence, in the presence of atomic hydrogen, most oxygen vacancies will form hydrogen complexes.

The metastable partner of the hydrogen bridge, denoted SiH + Si(3), is thermodynamically stable for all Fermi-level positions: by 0.16 eV in the positive charge state and by 0.6 eV in the negative charge state relative to the hydrogen bridge. Therefore this defect is present in

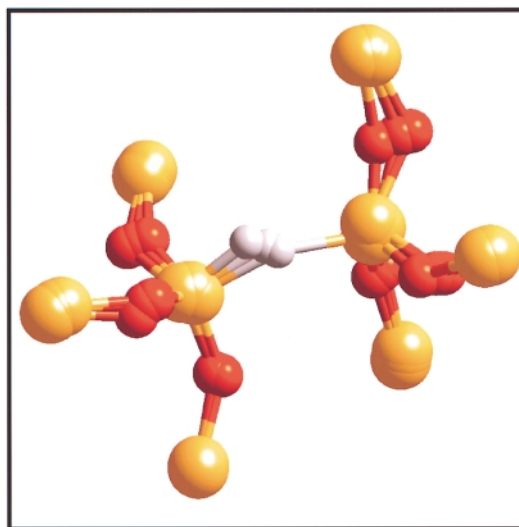


FIG. 3 (color). Overlaid structure of the hydrogen bridge in three charge states. Oxygen atoms are red, silicon atoms yellow, and hydrogen is white. The hydrogen position is located near the center of the bridge for the positive charge state, and localizes at one silicon as electrons are added.

larger concentrations. The neutral, EPR-visible form is the E_2' center [27], termed E_β' in an amorphous matrix. It contributes to the SILC at voltages above 3 eV, which is just below the energy at which electrons are introduced into the conduction band by direct tunneling.

We will now discuss how this prediction holds up against experimental evidence. Both defects are neutral traps as suggested by DiMaria and Cartier [9], i.e., the two charge states involved in the tunneling process are the neutral and negative charge states.

The electrically detected magnetic resonance (EDMR) spectra [28] exhibit a directionality, which has been explained by the direction of the current flow, if the defect has a well-defined axis such as a p -like orbital. This is clearly the case for the hydrogen bridge.

The g values observed by EDMR are 2.0022, with a shoulder at 2.0076 parallel to the axis of the current flow and one at 1.9997 perpendicular to it. E' centers could account for the main peaks. The shoulder at $g = 2.0076$ cannot be explained in terms of g values of known defects. We attribute the shoulder to the hydrogen hyperfine interaction of the E_4' center. It has an axial splitting of 2 mT [26] centered at $g = 2.0016$, in good agreement with the shoulder observed at ± 1 mT parallel to the current, and small equatorial splittings centered at $g = 2.0006$, corresponding to the absence of this shoulder for magnetic fields perpendicular to the current. The poorly resolved shoulder at 3462 G in the spectrum parallel to the electron flux could then correspond to the symmetric partner of the hyperfine line at lower magnetic field. The E_4' center alone, however, cannot explain the main peaks. As the experiment has been performed at 3 eV, the $E_\beta'(E_2')$ center can also contribute, which has only negligible hydrogen hyperfine interactions and g values at 2.0022 in the axial and 2.0006 in the equatorial directions [29]. Thus we attribute the spectrum to a superposition of two hydrogen complexes with the oxygen vacancy.

Tagaki *et al.* [30] directly measured an energy loss of 1.5 eV during SILC, in excellent agreement with our prediction of 1.7 eV for the hydrogen bridge.

In conclusion, we propose that the neutral hydrogen bridge is the trap mainly responsible for stress-induced leakage current through gate oxides. Charging this defect results in only minor structural distortions. The resulting small relaxation energy of 1.7 eV is required for tunneling at low voltages. Above 3.1 eV, another hydrogen-related silicon dangling-bond defect contributes to SILC. Existing experimental information supports the proposed microscopic model. Thus we have identified the origin of SILC, a forerunner of dielectric breakdown of gate oxides.

It is a pleasure to thank our colleagues A. Beck, J. G. Bednorz, G. L. Bona, R. Germann, W. Rieß, C. Rossel, H. W. M. Salemink, and D. Wiesmann for interesting discussions.

- [1] J. H. Stathis and D. J. DiMaria, in *IEDM '98 Technical Digest* (IEEE, Piscataway, 1998), p. 167.
- [2] D. L. Griscom, *J. Electron. Mater.* **21**, 762 (1992).
- [3] D. J. DiMaria, E. Cartier, and D. Arnold, *Appl. Phys. Lett.* **73**, 3367 (1993).
- [4] J. H. Stathis and E. Cartier, *Phys. Rev. Lett.* **72**, 2745 (1994).
- [5] E. Cartier, J. H. Stathis, and D. Buchanan, *Appl. Phys. Lett.* **63**, 1510 (1993).
- [6] R. E. Stahlbush, E. Cartier, and D. A. Buchanan, *Microelectron. Eng.* **28**, 15 (1995).
- [7] E. Cartier and J. H. Stathis, *Microelectron. Eng.* **28**, 3 (1995).
- [8] B. Ricco, M. Ya. Azbel, and N. M. Brodsky, *Phys. Rev. Lett.* **51**, 1795 (1983).
- [9] D. J. DiMaria and E. Cartier, *Appl. Phys. Lett.* **78**, 3883 (1995).
- [10] E. H. Nicollian, C. N. Berglund, P. F. Schmidt, and J. M. Andrews, *J. Appl. Phys.* **42**, 5654 (1971).
- [11] W. B. Fowler, J. K. Rudra, M. E. Zvanut, and F. J. Feigl, *Phys. Rev. B* **41**, 8313 (1990).
- [12] P. Hohenberg and W. Kohn, *Phys. Rev.* **136**, B664 (1964); W. Kohn and L. J. Sham, *Phys. Rev.* **140**, B1133 (1965).
- [13] J. P. Perdew and Y. Wang, *Phys. Rev. B* **45**, 13244 (1992); J. P. Perdew, K. Burke, and M. Ernzerhof, *Phys. Rev. B* **46**, 6671 (1992).
- [14] P. E. Blöchl, *Phys. Rev. B* **50**, 17953 (1994).
- [15] Augmented plane waves are included up to a cutoff of $E_{pw} = 30$ Ry, and the density is expanded up to 60 Ry.
- [16] K. G. Druijff, J. M. M. de Nijs, E. van der Drift, E. H. A. Granneman, and P. Balk, *Microelectron. Eng.* **22**, 231 (1993).
- [17] A. Yokozawa and Y. Miyamoto, *Phys. Rev. B* **55**, 13783 (1997).
- [18] F. J. Himpsel, F. R. McFeely, A. Taleb-Ibrahimi, J. A. Yarmoff, and G. Hollinger, *Phys. Rev. B* **38**, 6084 (1988).
- [19] E. H. Pointdexter and W. L. Warren, *J. Electrochem. Soc.* **142**, 2508 (1995).
- [20] J. K. Rudra and W. B. Fowler, *Phys. Rev. B* **35**, 8223 (1987).
- [21] D. C. Allan and M. P. Teter, *J. Am. Ceram. Soc.* **73**, 3247 (1990).
- [22] K. C. Snyder and W. B. Fowler, *Phys. Rev. B* **48**, 13238 (1993).
- [23] M. Boero, A. Pasquarello, J. Sarnthein, and R. Car, *Phys. Rev. Lett.* **78**, 887 (1997).
- [24] R. A. Weeks, *J. Appl. Phys.* **27**, 1376 (1956).
- [25] M. G. Jani, R. B. Bossoli, and L. E. Halliburton, *Phys. Rev. B* **27**, 2285 (1983).
- [26] J. Isoya, J. A. Weil, and L. E. Halliburton, *J. Chem. Phys.* **74**, 5436 (1981).
- [27] J. K. Rudra, W. B. Fowler, and F. Feigl, *Phys. Rev. Lett.* **55**, 2614 (1985).
- [28] J. H. Stathis, *Appl. Phys. Lett.* **68**, 1669 (1996).
- [29] D. L. Griscom, *Nucl. Instrum. Methods Phys. Res., Sect. B* **1**, 481 (1984).
- [30] S. Tagaki, N. Yasuda, and A. Toriumi, in *IEDM '96 Technical Digest* (IEEE, Piscataway, 1996), p. 323.